

An observational proxy of halo assembly time and its correlation with galaxy properties

S.H. Lim^{1*}, H.J. Mo¹, Huiyuan Wang² and Xiaohu Yang^{3,4}

¹*Department of Astronomy, University of Massachusetts, Amherst MA 01003-9305, USA*

²*Key Laboratory for Research in Galaxies and Cosmology, University of Science and Technology of China, Hefei, Anhui 230026, China*

³*Center for Astronomy and Astrophysics, Shanghai Jiao Tong University, Shanghai 200240, China*

⁴*IFSA Collaborative Innovation Center, Shanghai Jiao Tong University, Shanghai 200240, China*

Accepted Received; in original form

ABSTRACT

We show that the ratio between the stellar mass of central galaxy and the mass of its host halo, $f_c \equiv M_{*,c}/M_h$, can be used as an observable proxy of halo assembly time, in that galaxy groups with higher f_c assembled their masses earlier. Using SDSS groups of Yang et al., we study how f_c correlates with galaxy properties such as color, star formation rate, metallicity, bulge to disk ratio, and size. Central galaxies of a given stellar mass in groups with $f_c > 0.02$ tend to be redder in color, more quenched in star formation, smaller in size, and more bulge dominated, as f_c increases. The trends in color and star formation appear to reverse at $f_c < 0.02$, reflecting a down-sizing effect that galaxies in massive halos formed their stars earlier although the host halos themselves assembled later (lower f_c). No such reversal is seen in the size of elliptical galaxies, suggesting that their assembly follows halo growth more closely than their star formation. Satellite galaxies of a given stellar mass in groups of a given halo mass tend to be redder in color, more quenched in star formation and smaller in size as f_c increases. For a given stellar mass, satellites also tend to be smaller than centrals. The trends are stronger for lower mass groups. For groups more massive than $\sim 10^{13}M_\odot$, a weak reversed trend is seen in color and star formation. The observed trends in star formation are qualitatively reproduced by an empirical model based on halo age abundance matching, but not by a semi-analytical model tested here.

Key words: methods: statistical – galaxies: evolution – galaxies: formation – galaxies: haloes.

1 INTRODUCTION

In the current standard Λ CDM model, dark matter halos form through gravitational instability - induced hierarchical clustering, and galaxies are believed to form at the centers of dark matter halos through cooling and condensation of baryonic gas (e.g. Mo et al. 2010, for a review). The formation and evolution of galaxies are, therefore, expected to be closely linked to the assembly history of their host halos. There have been continuous efforts to establish the connections between galaxies of different properties and dark matter halos using empirical models, such as halo occupation distribution (HOD) (e.g. Jing et al. 1998; Peacock & Smith 2000; Seljak 2000; Scoccimarro et al. 2001; Berlind & Weinberg 2002; Zheng et al. 2007; Leauthaud et al. 2012; Watson et al. 2012), conditional luminosity function (CLF) (Yang et al. 2003; van den Bosch et al. 2007), and halo abundance

matching (HAM) (Mo et al. 1999; Kravtsov et al. 2004; Vale & Ostriker 2004, 2006; Conroy & Wechsler 2009; Guo et al. 2010; Neistein et al. 2010; Watson et al. 2012; Kravtsov 2013). The CLF and HOD models assign galaxies into dark matter halos predicted by a given cosmology, so that the predicted galaxy population matches the observed luminosity (stellar mass) functions and spatial clustering properties of galaxies. The HAM approach, on the other hand, populates galaxies into halos and sub-halos, assuming that there is a roughly monotonic correspondence between the ranking orders of the luminosities (or stellar masses) of galaxies and those of the masses of dark matter halos.

Most of the studies based on these approaches have so far focused on using the mass of halos to link galaxies with halos, thus implicitly assuming that galaxy properties are determined by halo mass alone. In reality, however, other properties of halos, such as assembly history, spin, and shape, may also play an important role in galaxy formation and evolution. These halo properties, therefore, should also

* E-mail: slim@astro.umass.edu

be used in understanding the relationships between galaxies and halos.

In this paper, we investigate how the properties of galaxies of a given stellar mass are correlated with the assembly time of their host halos. To this end, we propose an observational proxy of halo assembly time motivated by the results of Wang et al. (2011). Using high-resolution N -body simulations, Wang et al. investigated a large number of halo properties, such as formation time, substructure fraction, spin and shape, and their correlations among themselves and with large scale environments. Most of these halo properties are, unfortunately, not directly observable, and so it is difficult to test directly their effects on galaxy formation with observational data. One exception is the sub-structure fraction, which is defined as $f_s = 1 - (M_{\text{main}}/M_h)$, where M_h is the mass of the halo, and M_{main} is the mass of the main sub-halo located at the center of the host halo. This quantity is found to be correlated tightly with many other halo properties, in particular the formation time, spin and shape. More importantly, this quantity may be estimated from observations. Indeed, with a well-defined galaxy system, such as a galaxy group selected with the halo-based group finder of Yang et al. (2005), a good proxy of M_{main} is $M_{*,c}$, the stellar mass of the central galaxy in a group according to halo-galaxy abundance matching, and M_h can be estimated from the total stellar mass of the group, as demonstrated in Yang et al. (2005, 2007). Thus, one can use $f_c \equiv M_{*,c}/M_h$ as an observational proxy of the assembly time of the host halo of the group, and study how galaxy properties change with f_c . The goal of the present paper is to use this proxy to study the correlations between galaxy properties and the assembly time of their host groups (halos).

This paper is organized as follows. In Section 2, we describe the observational galaxy catalogs from which our galaxy and group samples are selected. In Section 3 we demonstrate how f_c can be used as a reliable proxy of halo assembly time. Detailed analyses of the correlations between galaxy properties and f_c of their host groups are presented in Section 4, and a preliminary comparison of our results with models is made in Section 5. Finally, in Section 6, we summarize our main conclusions.

2 OBSERVATIONAL DATA

2.1 SDSS galaxies

The galaxy samples used in this paper are obtained from the Sloan Digital Sky Survey (SDSS). Specifically, the galaxy catalog, as described in Wang et al. (2012) (W12 hereafter) and publicly available at <http://gax.shao.ac.cn/data/Group.html>, is constructed from the New York University Value-Added Galaxy Catalogue (NYU-VAGC; Blanton et al. 2005), which is based on SDSS Data Release 7 (SDSS DR7; Abazajian et al. 2009), but updated with a set of improvements over the original pipeline. From this catalog, we select all galaxies in the Main Galaxy Sample with extinction-corrected apparent r -band magnitude brighter than 17.72, with redshifts in the range $0.01 \leq z \leq 0.20$, and with redshift completeness $C_z > 0.7$. This leaves 639,359 galaxies in total, with a sky coverage of 7,748 deg². Of these, 599,301 galaxies have redshifts from the SDSS DR7,

2,450 galaxies with redshifts from the 2dFGRS (Colless et al. 2001), 819 with redshifts from the Korea Institute for Advanced Study Value-Added Galaxy Catalogue (KIAS-VAGC; e.g. Choi et al. 2010), 36,759 galaxies with redshifts from their nearest neighbors (since they do not have spectroscopic redshift measurements due to fiber collisions), and 30 galaxies with redshifts from ROSAT X-ray clusters. We exclude galaxies with assigned redshifts that have $^{0.1}M_r - 5 \log h \leq -22.5$ to prevent fiber-collided galaxies with real redshifts much lower than the nearest neighbors so that their luminosities are vastly over-estimated. The catalog also contains, for each galaxy, the $(g-r)$ and other colors, which are all $K + E$ -corrected to $z = 0.1$. In the following, this catalog will be referred to as the SDSS DR7 catalog to distinguish it from other catalogs we use in our study.

For all galaxies, we adopt stellar masses (M_*) from the data release of Brinchmann et al. (2004), available at <http://www.mpa-garching.mpg.de/SDSS/DR7/>. The data release also provides star formation rates (SFRs), and specific star formation rates (sSFRs, defined to be SFR divided by M_*). The SFRs are obtained by fitting the SDSS spectra with a spectral synthesis model. Specifically, H α luminosities are used for star forming galaxies and the D4000 breaks are used for galaxies without significant emission lines. Gas phase metallicities [for example, oxygen abundance, in terms of $\log(\text{O}/\text{H})$] are also available for a fraction of the galaxies, as described in Tremonti et al. (2004). In total, about 6% of the galaxies in the SDSS DR7 catalog are missing in the Brinchmann et al. data release, most of which are fiber-collided galaxies missing spectra. The number of galaxies for which a given quantity is actually available varies from quantity to quantity. For example, gas phase metallicity is available only for emission line galaxies.

2.2 Disk-bulge decomposition

We also make use of the results of Simard et al. (2011) obtained from bulge-disk decompositions of galaxies, which fit each galaxy image with the sum of a pure exponential disk and a de Vaucouleurs bulge using GIM2D. The code returns parameters such as the total flux, the bulge to total ratio B/T , the bulge half-light radius R_{50} and the disk scale length R_{disk} . In this paper we use the results based on the r -band images. About 92% of our SDSS DR7 galaxies can be cross identified in Simard et al.'s data base.

2.3 Information from the Galaxy Zoo

The Galaxy Zoo is a project in which volunteers are asked to classify images of over 900,000 SDSS DR7 galaxies into six morphological categories. The Galaxy Zoo 2 (GZ2 hereafter; Willett et al. 2013), the successor of the original Galaxy Zoo, continued the spirit of the original project but asking volunteers much more detailed morphological questions such as the number of spiral arms, tightness of the arms, etc. To enable such detailed questions, GZ2 uses a subsample of the brightest 25% of the resolved galaxies in the SDSS North Galactic Cap region within the redshift range of $0.0005 < z < 0.25$ along with a few more selection criteria (see Willett et al. 2013). This leaves a grand total of 245,609 SDSS DR7 galaxies.

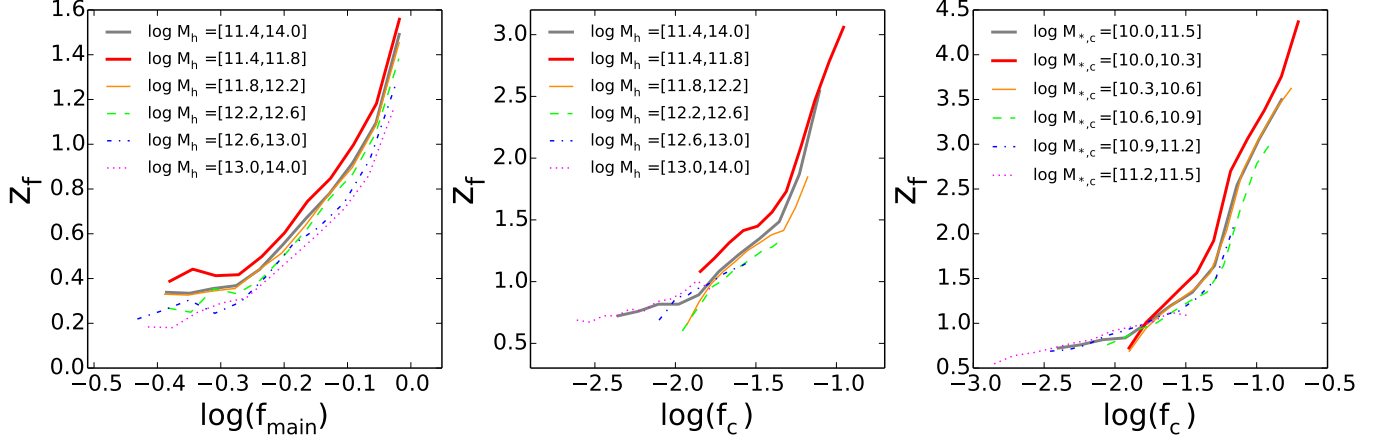


Figure 1. A demonstration how f_c can be used as a proxy of halo assembly time. *Left* : The correlation between half-mass assembly time z_f and $f_{\text{main}} = M_{\text{main}}/M_h$ (median) obtained from N -body simulations, based on data published in W11, where M_{main} is the mass of the most massive sub-halo in each host halo. Results are shown for halos in five mass ranges, as indicated. For comparison, the result for the total halo sample is shown as the gray line. *Middle* : The correlation between z_f and $f_c \equiv M_{*,c}/M_h$ (median), where $M_{*,c}$ is the stellar mass of the central (most massive) galaxy, obtained from the mock galaxy catalog of Hearin & Watson (2013), constructed using an age abundance matching model combined with halos from the Bolshoi N -body simulation. Different curves denote different host halo mass bins, as indicated. The results for the total sample is shown as the gray line. *Right* : The same as the middle panel, except that different curves show different stellar mass bins of central galaxies, as indicated. Here again the result for the total sample is shown as the gray line for comparison.

The SDSS metadata for GZ2 (available at <http://data.galaxyzoo.org/>) adds a series of useful information for SDSS DR7 galaxies, in particular, morphological classifications made by volunteers' votes. Whenever 'ellipticals' or 'spirals' are seen in our following analyses, the classification is based on GZ2. Out of all galaxies cross-matched between SDSS DR7 and GZ2, 97,785 are ellipticals and 135,634 are spirals.

2.4 SDSS groups

Given that galaxy groups are defined as galaxies that reside in the same dark matter halo, galaxy groups can be used to directly probe the connections between galaxies and their host halos. Yang et al. (2005, 2007) have developed a halo-based group finder optimized for grouping galaxies in common dark matter halos. The performance of this group finder has been tested extensively using mock galaxy redshift surveys constructed from CLF models (Yang et al. 2003; van den Bosch et al. 2003; Yang et al. 2004) and from a semi-analytical model (Kang et al. 2005). It was found that this group finder is more successful than the traditional friends-of-friends (FoF) algorithm in grouping galaxies into their common dark matter haloes (see Yang et al. 2007, (Y07 hereafter)). The group finder performs consistently even for very poor systems such as isolated galaxies in small mass haloes, which enables its suitability to probe the galaxy-halo connection over a wide range of different haloes.

In the present paper, we use the DR7 group catalog, publicly available at <http://gax.shao.ac.cn/data/Group.html> to associate galaxies with groups. This catalog is made basically by applying exactly the same group finder of Y07 to SDSS DR7 galaxies. The details of the group finder is described in Y07. *WMAP5* cosmology was used to calculate distances from redshifts and to assign halo masses to selected

groups. We adopt the group catalog 'modelC', which uses model magnitudes rather than Petrosian magnitudes. For each group in the group catalog, the fraction, f_{edge} , of each group's volume that falls inside of the SDSS DR7 survey volume is given. Only groups with $f_{\text{edge}} \geq 0.6$ are used here, which removes about 1.6% of all groups.

The group halo masses M_h in the catalog are estimated using the ranking of groups either in the combined luminosity ($L_{19.5}$) or in the combined stellar mass (M_{stellar}) of all member galaxies with $^{0.1}M_r - 5 \log h \leq -19.5$. The conversion from $L_{19.5}$ or M_{stellar} to M_h is made by adopting the halo mass function of Tinker et al. (2008) and the method of abundance matching assuming one-to-one correspondence between $L_{19.5}$ (M_{stellar}) and M_h . As shown in Y07, while both $L_{19.5}$ and M_{stellar} are tightly correlated with M_h , the $M_h - M_{\text{stellar}}$ relation is slightly tighter, with a typical dispersion of ≈ 0.2 dex in M_h for a given M_{stellar} over the halo mass range considered here. We therefore use M_h based on M_{stellar} , although our tests showed that using $L_{19.5}$ does not change any of our results. For very small groups, no masses are assigned, and they are excluded from our analysis.

The identification of central galaxies for each group is also provided in two different ways: the brightest galaxy or the most massive galaxy in terms of stellar mass. In this study, we choose the latter as the definition of centrals.

3 AN OBSERVATIONAL PROXY OF HALO ASSEMBLY TIME

As mentioned in the introduction, Wang et al. (2011) (hereafter W11) explored the correlations among various halo properties using dark matter halos identified from high-resolution N -body simulations. One of the most important properties of a halo is its formation time, z_f , which is de-

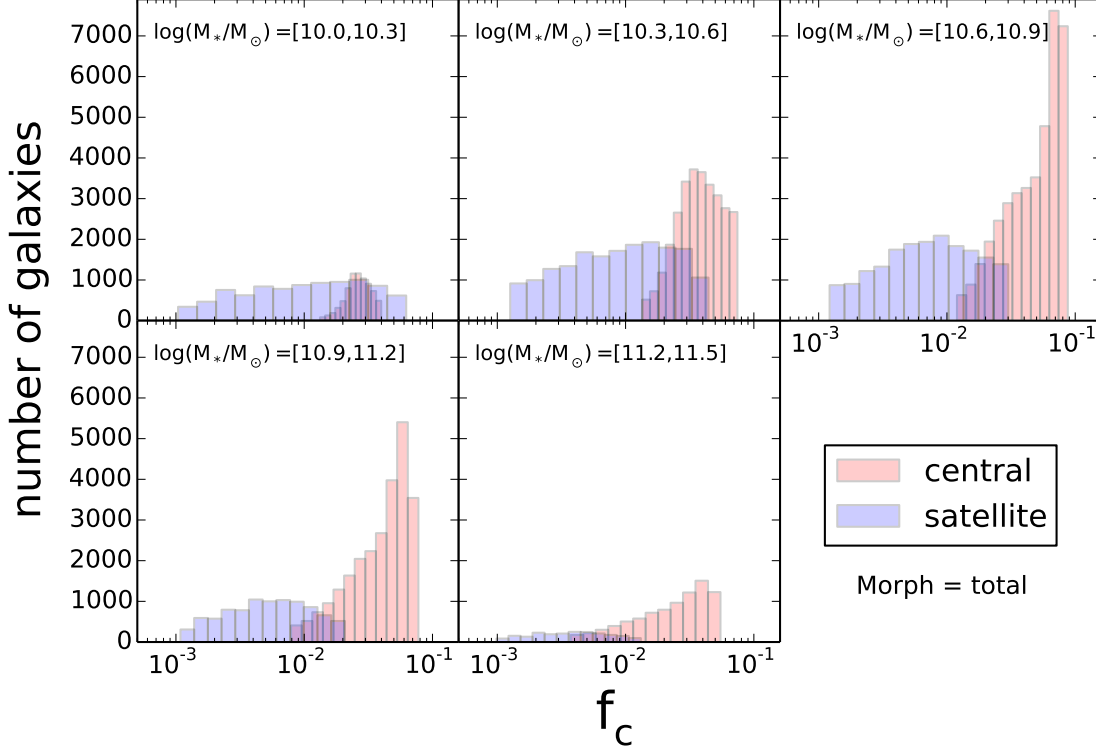


Figure 2. The number distribution of galaxies in f_c , with each panel corresponding to different stellar mass bins, as indicated on the top of each panel, for centrals (red) and satellites (blue).

finer to be the redshift at which the main progenitor of the halo has first assembled half of its final mass. This formation time is believed to have significant impact on the properties of the galaxies the halo hosts, such as galaxy age, color, star formation rate (SFR), etc. Unfortunately, z_f itself is not directly observable, and so it is not possible to examine the correlation between z_f of a halo and the properties of the galaxies the halo host. However, as shown in figure 1 of W11, and reproduced in the left panel of Figure 1, the halo formation time z_f shows a tight correlation with the substructure fraction, $f_s = 1 - f_{\text{main}}$ with $f_{\text{main}} = (M_{\text{main}}/M_h)$, where M_{main} is the mass of the main sub-halo at the center of each host halo, quite independent of the mass of the host halo. This suggests that f_{main} can be used as a proxy of z_f . Since M_h can be estimated for halos using halo abundance matching, as described in the previous section, and M_{main} can be estimated using sub-halo abundance matching, we can define an ‘observable’ quantity,

$$f_c \equiv \frac{M_{*,c}}{M_h}, \quad (1)$$

as a proxy of z_f . Here $M_{*,c}$ is the stellar mass of the central galaxy obtained from the rank of M_{main} . If there were no scatter in the halo-galaxy abundance matching, so that there is a one-to-one relation between galaxy stellar mass and sub-halo mass, $M_{*,c}$ would be a perfectly faithful indicator of M_{main} . By definition $M_{*,c}$ would also be the stellar mass

of the most massive galaxy in a group because the main sub-halo is the most massive one among all sub-halos. In reality, however, the halo mass - galaxy mass relation may not be one-to-one. Given this and that f_s is not perfectly correlated with z_f , f_c defined above can only be used as a proxy of z_f . As an illustration, the middle and right panels of Fig. 1 shows the correlation between z_f and f_c obtained from the HAM model of Hearin & Watson (2013) applied to dark matter halos in a high-resolution N -body simulation. As one can see, there is a tight correlation between f_c and z_f both for halos of a given mass (middle panel) and for centrals of a given stellar mass (right panel). In particular, the $z_f - f_c$ relation does not seem to depend strongly on halo mass or on galaxy mass, although massive systems extend further towards the low- f_c end because of the fact that $M_{*,c}$ only increases slowly with halo mass at the massive end (e.g. Yang et al. 2012). All these validate the use of f_c as an observational proxy of z_f .

In what follows we will examine how galaxy properties are correlated with f_c , and use the results to understand the connection between galaxy properties and halo assembly histories as represented by the formation redshift z_f . For reference, we show the distribution of galaxies in f_c for the entire SDSS DR7 sample in Figure 2. Each panel corresponds to a given stellar mass bin, as indicated in individual panels, and results are shown for both centrals and satellites. As expected, the centrals, defined to be the most massive ones

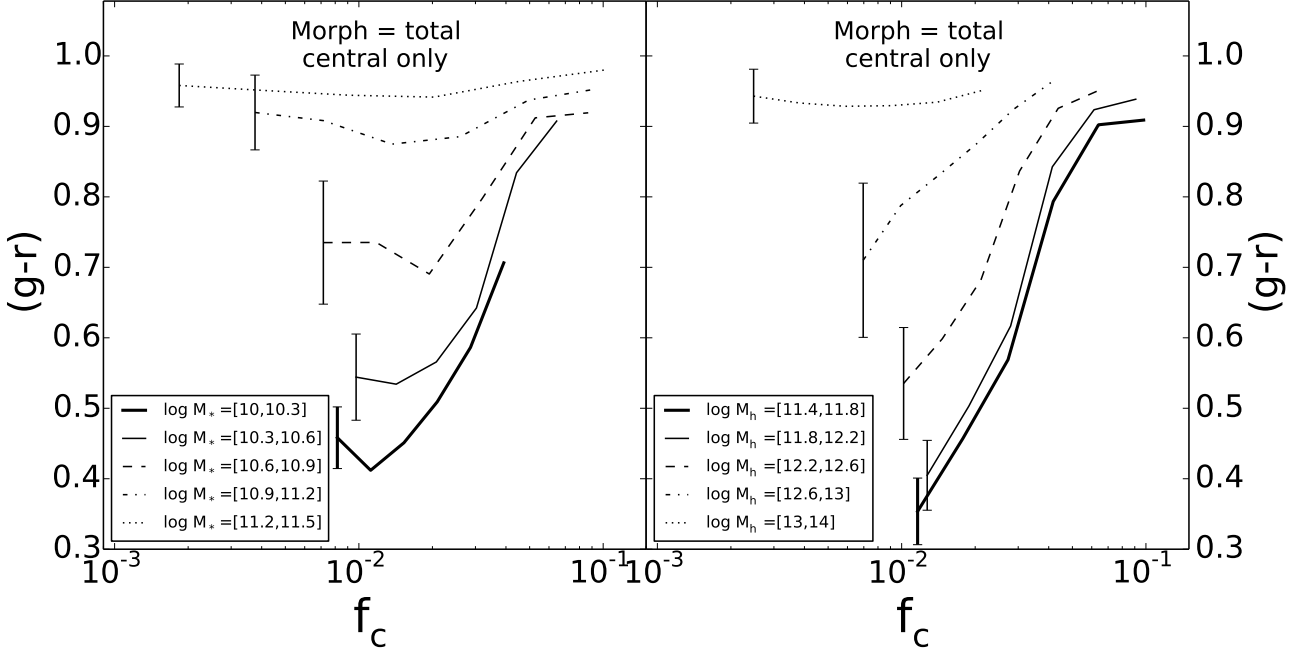


Figure 3. The correlation between $(g-r)$ color, $K+E$ corrected to $z=0.1$, and f_c , for centrals. The curves plot the median values in f_c bins. The error bars on the leftmost sides are ‘typical’ [16%, 84%] ranges for each mass bin. In the left panel different curves refer to galaxies in different stellar mass bins, as indicated, while in the right panel different curves are for galaxies residing in halos in different halo mass bins.

in groups, have on average a higher f_c value than satellites, since groups with lower f_c tend to have more satellites in them.

4 CORRELATION OF GALAXY PROPERTIES WITH f_c

This section examines the correlation of galaxy intrinsic properties with the value of f_c of the host group in which the galaxy resides. Results will be shown separately for central and satellite. While our presentation includes all groups, our test using only groups with more than one member galaxies brighter than $^{0.1}M_r - 5 \log h = -19.5$ gives qualitatively similar results.

4.1 Central galaxies

4.1.1 Color and star formation

Figure 3 shows the correlation between the $(g-r)$ color of central galaxies and f_c of their host groups. In the left panel, results are shown separately for galaxies in five different stellar mass ranges, as indicated in the inner panel, while in the right panel results are shown separately for five different halo mass bins. The lines are the median values within narrow f_c bins, while the bars present the typical [16%, 84%] range of the distribution in the corresponding halo mass or stellar mass range.

As one can see from the right panel, for a given halo mass, the $(g-r)$ color depends strongly on f_c , with centrals in halos with higher f_c being redder, except for the most massive halos, where the centrals are all equally red.

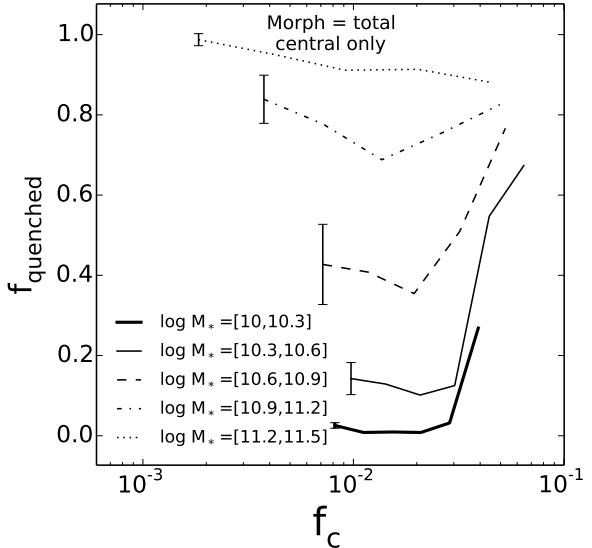


Figure 4. The correlation between the fraction of quenched galaxies and f_c for central galaxies. Quenched galaxies are defined to be the ones with star formation rate lower than the deviation line defined by equation (2). The curves plot the quenched fractions in f_c bins. Different curves refer to galaxies in different stellar mass bins, as indicated. The error bars here are ‘typical’ 1- σ dispersions among 100 bootstrap re-sampling.

Note that for halos with masses below $10^{12.6} M_\odot$, the dependence of color on halo mass is not strong for a given f_c . By definition, for a given halo mass, f_c is directly proportional

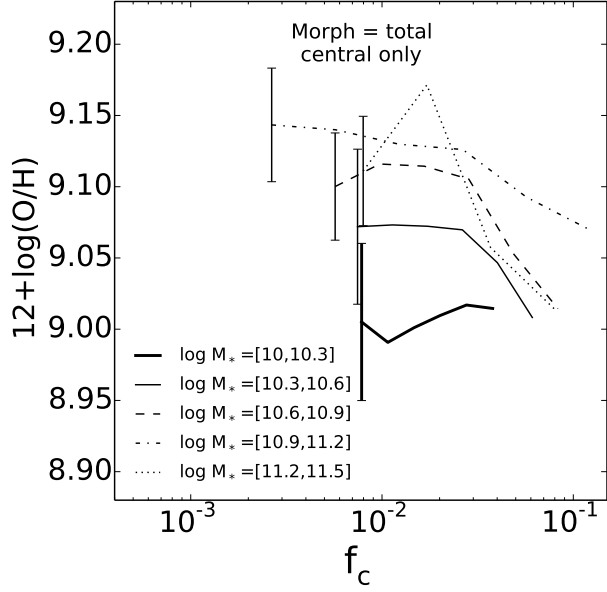


Figure 5. The correlation between gas phase oxygen abundance, $12 + \log(\text{O}/\text{H})$, and f_c for central galaxies. The curves plot the median values in f_c bins. The error bars on the leftmost sides are ‘typical’ [16%, 84%] ranges for each mass bin. Different curves refer to galaxies in different stellar mass bins, as indicated.

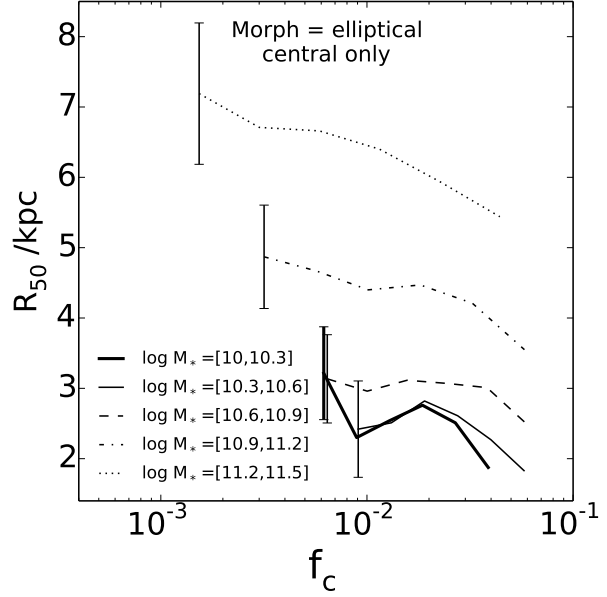


Figure 7. The correlation between the half-light radius (r -band) R_{50} and f_c for central ellipticals. The curves plot the median values in f_c bins. The error bars on the leftmost sides are ‘typical’ [16%, 84%] ranges for each mass bin. Different curves refer to galaxies in different stellar mass bins, as indicated.

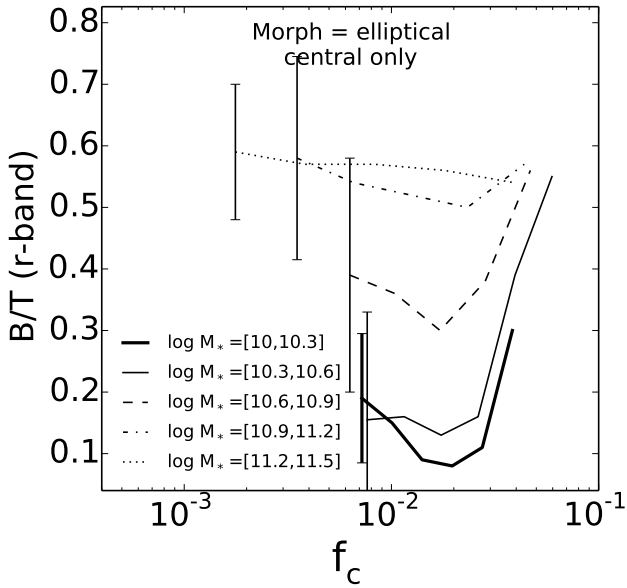


Figure 6. The correlation between the bulge to total ratio (in r -band), B/T , and f_c for central galaxies. The curves plot the median values in f_c bins. The error bars on the leftmost sides are ‘typical’ [16%, 84%] ranges for each mass bin. Different curves refer to galaxies in different stellar mass bins, as indicated.

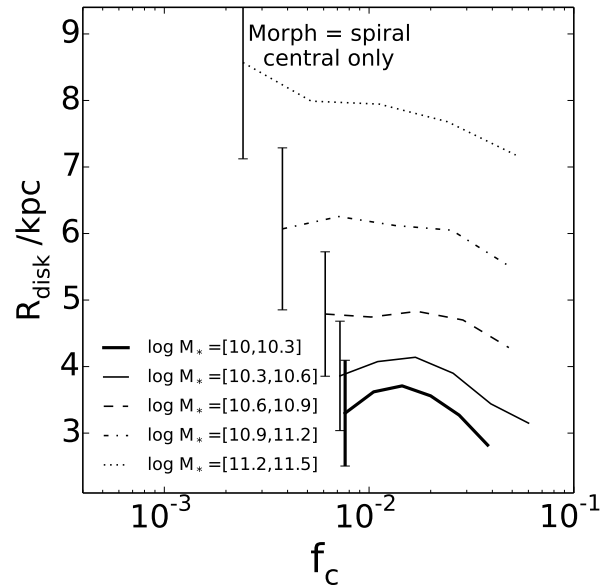


Figure 8. The correlation between disk scale length (r -band) R_{disk} and f_c for central spirals. The curves plot the median values in f_c bins. The error bars on the leftmost sides are ‘typical’ [16%, 84%] ranges for each mass bin. Different curves refer to galaxies in different stellar mass bins, as indicated.

to $M_{*,c}$, and it is well known that the intrinsic properties of galaxies depend strongly on their stellar mass. Thus, the strong dependence of color on f_c for a given halo mass bin see here is not surprising. However, given that f_c is strongly correlated with halo formation time (see Fig. 1), our results suggest that halo formation time may play an important

role in determining the color of the central galaxies. This is demonstrated more clearly in the left panel of Figure 3, where the $(g-r)$ color is shown as a function of f_c for centrals of fixed stellar mass. As one can see, massive galaxies are more or less all red, independent of f_c , while for galaxies with $M_* < 10^{11} M_\odot$, their colors depend strongly on f_c .

There seems to be a characteristic value $f_c \sim 0.01 - 0.02$, below and above which the color shows the opposite trends with f_c . At the high f_c end, galaxies become increasingly redder as f_c increases, which may be produced by the fact that groups with higher f_c on average assembled their halos earlier. In contrast, galaxies in groups with $f_c < 0.02$ seem to have a reversed, albeit weak, trend between color and f_c . Note that for a given central stellar mass, lower f_c corresponds to higher halo mass. The reversed trend at low f_c reflects a ‘down-sizing’ effect of massive halos, in that centrals in massive halos formed their stars earlier than in low mass halos (e.g. Lu et al. 2015), although the massive host halos themselves assembled (half of their masses) later (lower f_c). This is consistent with the fact that *in situ* star formation in massive halos is quenched once their masses reached a few times $10^{12}M_\odot$ (e.g. figure 14 of Lu et al. 2014b), and, for high mass halos, more massive ones on average assembled a fixed amount of mass earlier (Li et al. 2008).

Figure 4 shows the quenched fraction of centrals as a function of f_c . Because for a given halo mass, f_c and stellar mass is strongly degenerated for centrals, here and in the following we only show results for centrals divided into different stellar mass bins but not divided further according to halo mass. For galaxies in each stellar mass bin, we separate them into quenched and star forming sub-populations using the definition of Moustakas et al. (2013),

$$\log \left(\frac{\text{SFR}}{M_\odot \text{yr}^{-1}} \right) = -0.49 + 0.65 \log \left(\frac{M_*}{10^{10} M_\odot} \right) + 1.07(z - 0.1). \quad (2)$$

For a given M_* , galaxies with star formation rate (SFR) above the value given by the above equation are defined to be star forming, and those with SFR below the value are defined to be quenched. Given that the specific star formation rate (sSFR, defined as the ratio between SFR and M_*) of a galaxy is closely related to its color, it is not surprising that the general trends seen in this plot are similar to those shown in Fig. 3. Low-mass centrals are dominated by star forming galaxies in halos of low f_c but become dominated by quenched galaxies at the high end of f_c . A reversal of trend is again seen at $f_c \sim 0.02$.

Finally, let us look at the gas phase metallicity of galaxies, which is shown as a function of f_c in Figure 5. The gas phase metallicity estimates are available only for a limited fraction of galaxies, mostly star forming ones. The result for the highest stellar mass bin is quite noisy because here only a small fraction of galaxies are star forming. For a given stellar mass, there is a clear trend that the gas phase metallicity decreases with increasing f_c . For centrals with $M_* > 10^{10.3} M_\odot$, the decrease with f_c is quite rapid, by almost 0.1 dex. This decrease is comparable to the scatter in the gas phase metallicity - stellar mass relation obtained by Tremonti et al. (2004), suggesting that the scatter may be dominated by the variance in halo assembly, with galaxies formed in older dark matter halos tend to have lower gas-phase metallicities.

4.1.2 Structure and size

The bulge to total ratio, B/T , as described in the data section, is plotted against f_c in Figure 6. There are a number

of interesting trends. Overall, the B/T increases with stellar mass, simply owing to the fact that earlier type galaxies are on average more massive. For massive galaxies with M_* higher than about $10^{11} M_\odot$, the B/T ratio on average decreases with f_c . For galaxies with lower stellar masses, the trend changes at $f_c \sim 0.02$. While the B/T ratio decreases with increasing f_c at the low f_c end, it increases with f_c rapidly at $f_c > 0.02$.

As mentioned above, for a given central mass $M_{*,c}$, a lower f_c on average corresponds to a higher halo mass M_h . Since a higher halo mass on average corresponds to a higher group richness, the decline of B/T with f_c may, therefore, be understood in terms of the morphology-density relation found by Dressler (1980) that early-type galaxies (higher B/T) are preferentially found in high density environments, while late-type galaxies are more likely to be found in poor groups and in the lower density fields. The increase of B/T with decreasing f_c at the low f_c end shown in Fig. 6 follows such a morphology-density relation. However, our results also contain new information, in that the morphology-density relation is present even for centrals of a given stellar mass.

The strong increase of B/T with increasing f_c seen for low-mass central galaxies with $M_* < 10^{11} M_\odot$ at $f_c > 0.02$ runs against the morphology-density relation. Since larger f_c means an earlier assembly time, as shown in the last section, the trend of B/T with f_c indicates an dependence on halo assembly time, in that central galaxies in older halos tend to have higher B/T . In the current CDM paradigm of structure formation, the formation of halos of a given mass at earlier time is on average more dominated by major mergers and older halos are on average more compact (e.g. Li et al. 2007; Zhao et al. 2009). If the bulge components are formed through major mergers or through secular evolutions of the disk components, their formation is expected to be promoted by both major mergers and a compact structure of dark matter halos. The positive correlation between B/T and f_c obtained here may follow directly from such formation. The reversal of the trend at $f_c < 0.02$ is also consistent with such interpretation, because central galaxies in massive halos actually have earlier formation due to the down-sizing effect described above.

Figures 7 and 8 show how the sizes of central galaxies of a given stellar mass correlate with f_c . Results are shown separately for the half-light radius (R_{50}) of ellipticals and the disk scale-length (R_{disk}) of spiral galaxies. Here the morphological separation is made according to the visual classification from GZ2, and the sizes are taken from the r -band bulge-disk decompositions of Simard et al. (2011). For both ellipticals and spirals, more massive galaxies are larger, as expected. For a given stellar mass, the sizes of centrals decrease with f_c at $f_c > 0.02$. This is consistent with the interpretation that halos formed earlier on average are smaller. However, unlike star formation, there is no strong reversal of trend at $f_c < 0.02$, in particular for massive galaxies. For elliptical galaxies, this may be due to the fact that the assembly of the stellar component follows halo assembly more closely than star formation (e.g. figure 5 in Lu et al. 2015). For spiral galaxies, this result may indicate that disks can continue to accrete cold gas from halos as the halos grow, even in relatively massive systems.

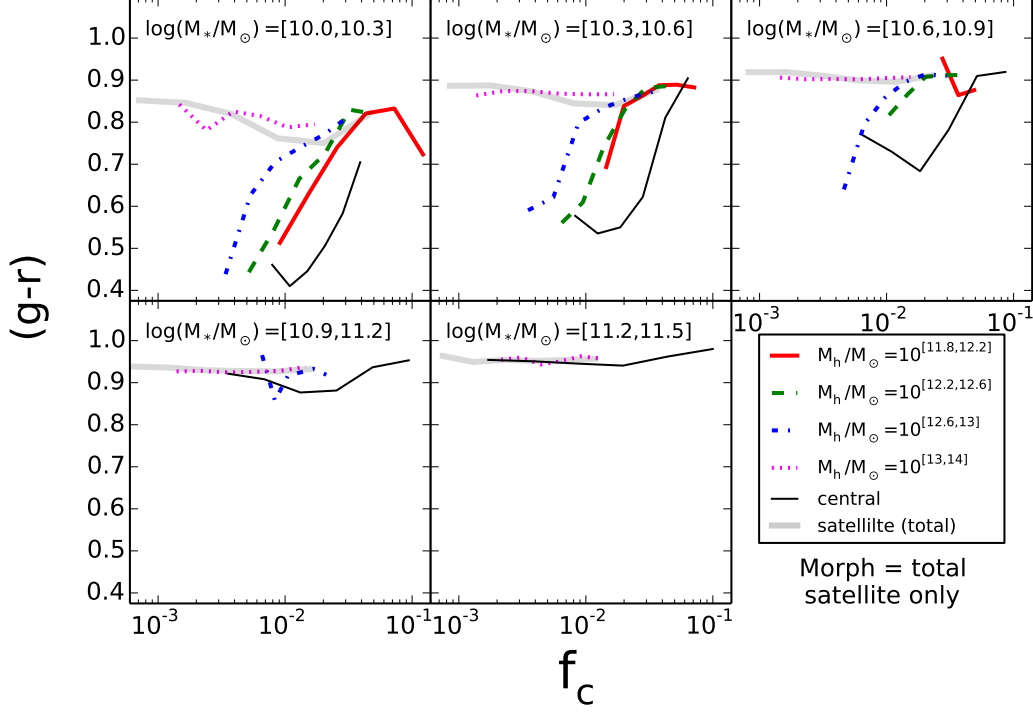


Figure 9. The correlation between $(g-r)$ color and f_c for satellite galaxies (thick lines). Individual panels show the medians in f_c bins for satellites of different stellar masses. Within each panel, satellites are divided into four subsamples according to the masses of their host halos, as denoted in the legend. The result for the total satellite sample in a given stellar mass bin is shown as the translucent thicker line in each panel. For comparison medians for centrals shown in Fig. 3 are re-plotted here as the thin solid lines.

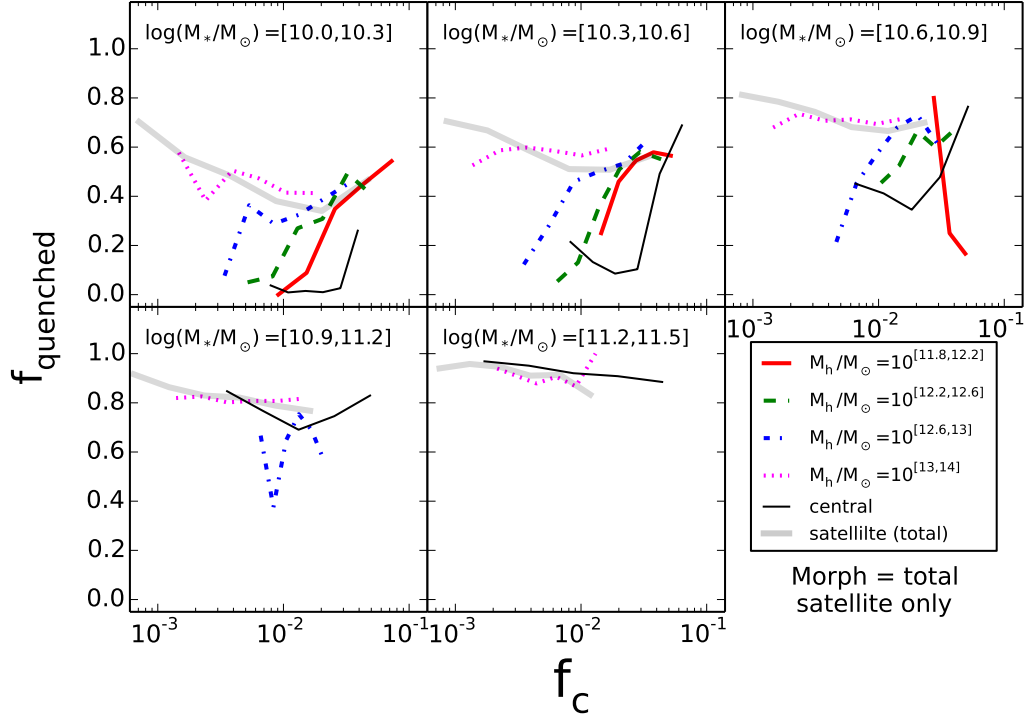


Figure 10. The correlation between the quenched fraction and f_c for satellite galaxies (thick lines). Individual panels show the medians in f_c bins for satellites of different stellar masses. Within each panel, satellites are divided into four subsamples according to the masses of their host halos, as denoted in the legend. The result for the total satellite sample in a given stellar mass bin is shown as the translucent thicker line in each panel. For comparison medians for centrals shown in Fig. 4 are re-plotted here as the thin solid lines.

4.2 Satellite galaxies

Figure 9 shows the $(g - r)$ color of satellite galaxies as a function of f_c of their host groups. The five panels show the results of galaxies in five stellar mass bins, as indicated. For each stellar mass bin, results are shown separately for galaxies in groups of four different halo mass bins, as indicated in the small panel. For given f_c and halo mass, more massive galaxies on average are redder. For the most massive galaxies with $M_* > 10^{11} M_\odot$, which are only found in massive halos, their $(g - r)$ colors are all red, quite independent of f_c . For satellites with lower stellar masses ($M_* < 10^{11} M_\odot$), there is a marked trend that the $(g - r)$ color becomes increasingly redder as f_c increases. The trend is weaker for groups with higher halo masses, and becomes almost totally flat for halo masses above $\sim 10^{13} M_\odot$ (the magenta dotted curve in each panel). We do not see a reversal in the trend in any ranges of f_c as seen in central galaxies shown in Fig. 3 (reproduced here as the black solid curves for comparison), because here results are shown separately for groups in different halo mass bins. If we consider all satellites of a given stellar mass regardless of their host halo mass, then we get the results as shown by the thick shaded line in each panel. Here we do see a change of trend at $f_c \sim 0.02$, which is similar to, albeit weaker than that for central galaxies. Clearly, satellites at the low- f_c end are dominated by the ones in massive groups. The reversed trend at $f_c < 0.02$, is consistent with the fact that galaxies in massive halos actually have earlier formation due to the down-sizing effect described earlier.

Figure 10 shows the quenched fraction of satellites as a function of f_c of their host groups. The format of this figure is exactly the same as Fig. 9, and the quenched fraction is again determined by using equation (2). The trends shown here are very similar to those in Fig. 9, again because the $(g - r)$ color is closely correlated with the sSFR used to separate quenched from star-forming galaxies.

Finally let us look at the sizes of galaxies. Here we consider ellipticals and spirals separately. Our tests showed that the dependence of size on halo mass is weak for satellites and the current samples are too small to give significant results for the halo-mass dependence. Thus, we only divide galaxies into stellar mass bins, but not further into halo mass bins. Figures 11 and 12 show how the sizes of satellite galaxies of a given stellar mass correlate with f_c (thick solid curves). Here results are shown separately for the half-light radius (R_{50}) of ellipticals and the disk scale-length (R_{disk}) of spiral galaxies, both taken from the r -band bulge-disk decompositions of Simard et al. (2011). For both ellipticals and spirals, the trend with f_c is rather weak, although for low-mass galaxies the size seems to decrease as one moves away from $f_c \sim 0.01$ toward both the low and high ends of f_c . This trend suggests that galaxies of a given stellar mass on average have smaller sizes if formed earlier.

Compared with central galaxies of the same stellar mass (shown by the thin curves), satellites are smaller. This is true for both spirals and ellipticals, and the difference is larger for lower mass galaxies. It is interesting to note that the average sizes of satellites are comparable to those of centrals with the highest f_c , which indicates that sub-halos which host satellites may have as early formation as the oldest halos of similar masses that host centrals.

Weinmann et al. (2009) found that, at fixed stellar mass,

late-type satellite galaxies have smaller radii than late-type central galaxies. Our results confirm theirs. However, Weinmann et al. (2009) found no difference in size for early-type galaxies, while Fig. 11 shows clearly that such difference also exists for ellipticals, particularly for ellipticals with low stellar masses. The discrepancy may arise from the difference in the separation of early versus late types. While Weinmann et al. (2009) used the concentration parameter, defined as the ratio between R_{90} (radius within which 90% of the total light is included) and R_{50} , we use morphological classifications from GZ2. Weinmann et al. (2009) interpreted their finding as owing to the fading of stellar disks due to the aging of stars. However, it is unclear if such an interpretation can also explain the systematic change of disk size of central galaxies with f_c . Passive stellar evolution alone is also difficult to explain the difference between centrals and satellites for elliptical galaxies. Based on our results, the more likely reason is that halos formed earlier are more compact, and that the difference in sizes between centrals and satellites is due to differences in formation time, just as centrals in halos of different f_c .

5 COMPARISON WITH MODELS

In order to explore the implications of our findings, we make comparisons of our results with some theoretical models. Since our results are derived from galaxy groups selected from a redshift catalogue, a detailed comparison between our observational results with theoretical models requires the construction of theoretical mock catalogs that take into account all observational selection effects. This is beyond the scope of this paper, and we will come back to this in a forthcoming paper. In this paper, we use halo occupations of galaxies predicted directly by models, ignoring all observational selection effects. As a demonstration, we use two specific models: the empirical age abundance matching (AAM) model published in Hearin & Watson (2013); Hearin et al. (2014), and the semi-analytical model (SAM) as described in Lu et al. (2014a).

While traditional abundance matching techniques only exploit the correlation between luminosity of galaxies and mass of their host haloes to assign galaxies in haloes from simulations, the AAM connects galaxies to haloes as a function of both color and luminosity. Specifically, it assigns stellar masses to galaxies according to the mass ranking of their host halos, and assign colors to galaxies of a given stellar mass according to the formation time ranking of their halos. The SAM approach, on the other hand, attempts to model physical processes using simplified receipts parameterized in simple functional forms. A SAM generally contains a large number of free parameters. Lu et al. (2014a) used a Monte Carlo Markov Chain method to infer their model parameters from observational constraints such as luminosity functions of galaxies at different redshifts. The Lu et al. SAM contains many of the same components as other SAMs. In particular it assumes a strong star formation feedback and an efficient gas stripping to prevent too much star formation in dark matter halos.

Since none of the models provides reliable predictions for the structural properties of galaxies, here we focus only on the star formation properties as represented by the spe-

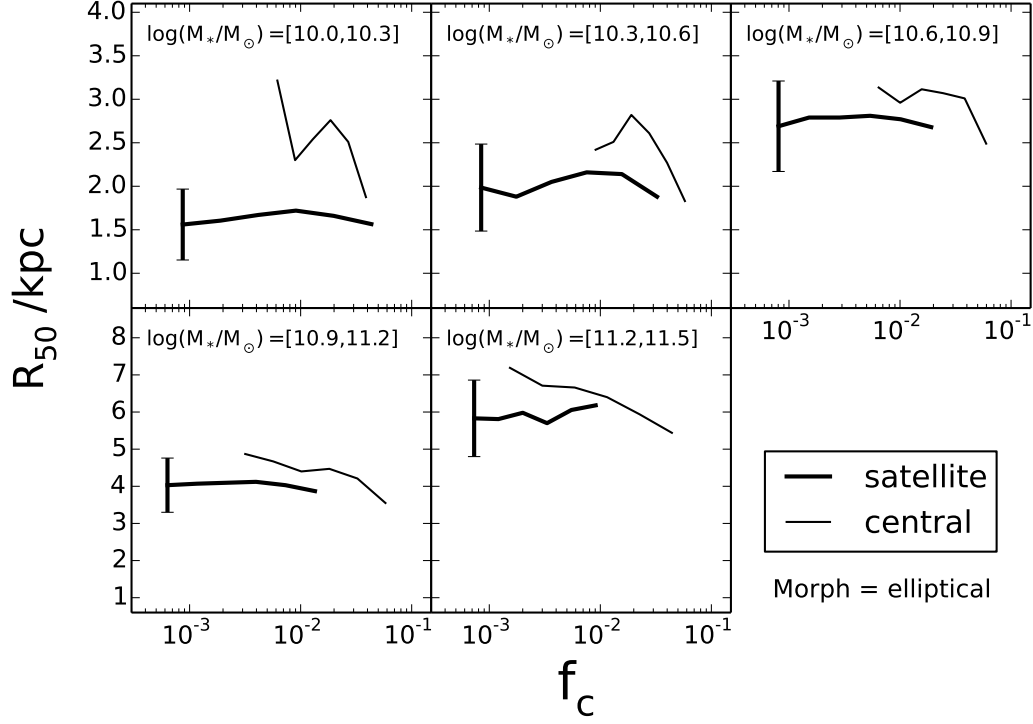


Figure 11. The correlation between R_{50} and f_c for satellite ellipticals. The thick curves are the medians in f_c bins, while the ‘typical’ [16%, 84%] ranges are indicated by the bars on the leftmost sides. For comparison, results for central ellipticals shown in Fig. 7 are re-plotted here as thin lines. Different panels show the results in different stellar mass bins, as indicated.

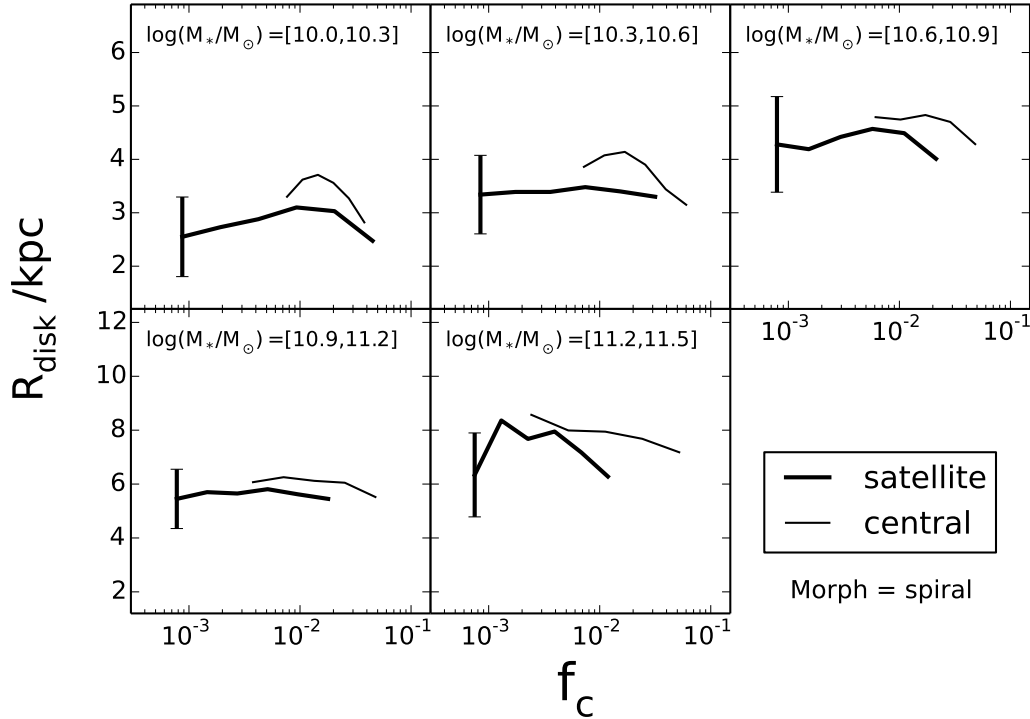


Figure 12. The correlation between R_{disk} and f_c for satellite spirals. The thick curves are the medians in f_c bins, while the ‘typical’ [16%, 84%] ranges are indicated by the bars on the leftmost sides. For comparison, results for central spirals shown in Fig. 8 are re-plotted here as thin lines. Different panels show the results in different stellar mass bins, as indicated.

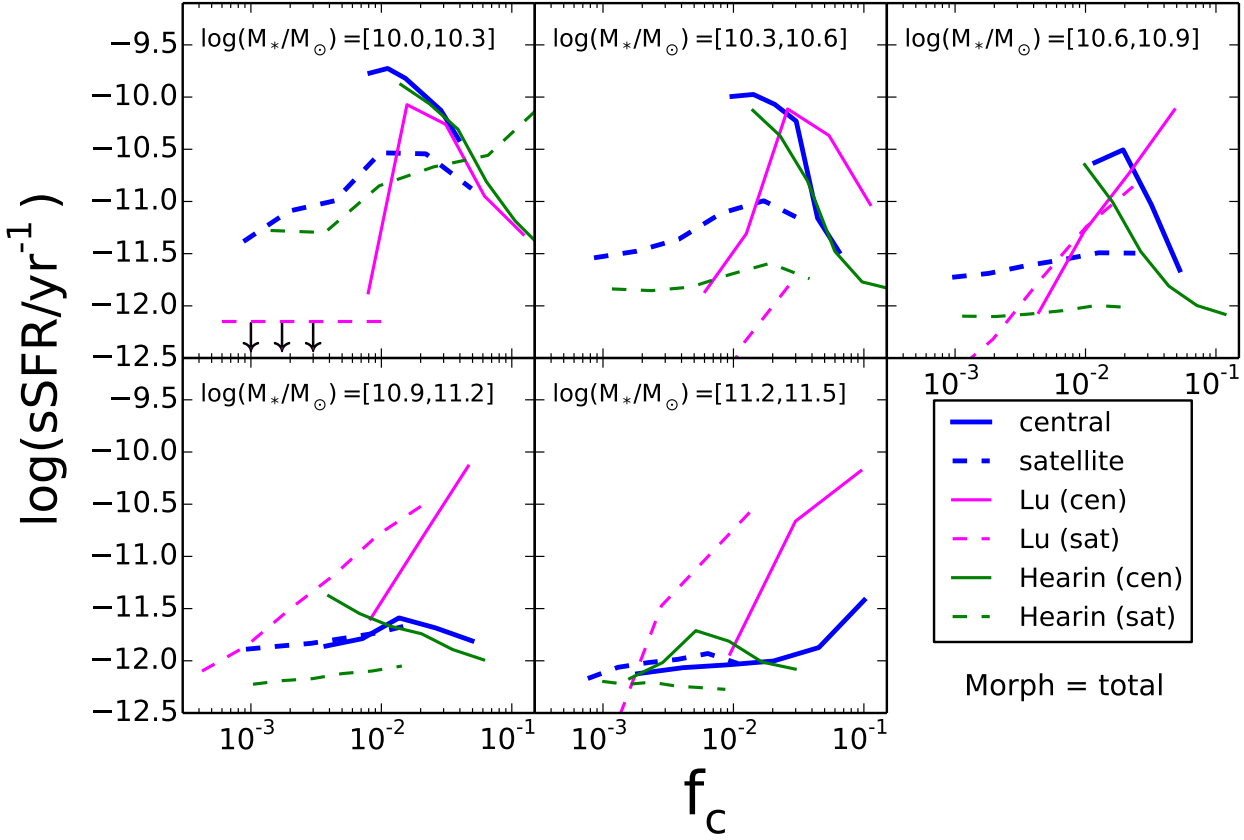


Figure 13. The observed correlation between f_c and the specific star formation rate, sSFRs (blue lines: solid for centrals and dashed for satellites) in comparison to the predictions of the semi-analytical model (SAM) of Lu et al. (2014a) (thin magenta) and the age abundance matching model of Hearin & Watson (2013) (thin green). Note that the sSFR of satellites in the first panel for the SAM are too low to show, and are represented by a horizontal line with down pointing arrows.

cific star formation rate (sSFR) of galaxies. Figure 13 shows the sSFR as a function of f_c as predicted by the models of Hearin & Watson (2013) and Lu et al. (2014a). As in the observation, we identify the most massive galaxy in a halo to be the central galaxy, and use the ratio between $M_{*,c}$ and the halo mass to define f_c . Here results are shown separately for centrals and satellites in five different stellar mass bins. For comparison, our observational results are included in each panel. As one can see, the AAM model reproduces the observational trends qualitatively. In particular, the rapid decreases of sSFR with increasing f_c for central galaxies in the low stellar mass bins are well reproduced. The trends for satellite galaxies are also well produced, although the predicted sSFR are systematically lower than the observational results. This discrepancy should not be taken too seriously, as the satellite population in observational groups may be contaminated by centrals that on average have higher SFR than the satellites of the same mass. As mentioned above, such contaminations can only be taken into account properly by applying the same group finder to the mock catalog constructed from the AAM model.

In contrast, the predictions of the SAM are very different from the observational results. The model predicts too much quenching of star formation in low mass satellites, while the star formation rates in centrals, particularly

in groups with high f_c , are over-predicted by more than an order of magnitude. The SAM also fails to catch the overall trends in the observation, even qualitatively. These results suggest that the halo assembly plays an important role in regulating star formation, and the underlying physical processes are still poorly captured in the SAM considered here. It is clearly interesting to compare our results with other SAMs and simulation results, not only in sSFR, but also in other properties, such as size, B/T , and metallicity, to explore the implications of our results.

6 SUMMARY

We have showed that the ratio, $f_c \equiv M_{*,c}/M_h$, can be used as a reliable observational proxy of halo assembly time, with higher f_c for halos that assembled earlier. This use was motivated by the results of W11, who used N-body simulations to show that there is a tight correlation between M_{main}/M_h (M_{main} being the main sub-halo mass) and halo half-mass assembly redshift (z_f), combined with (sub)halo abundance matching. We used the SDSS groups by Yang et al. to investigate how galaxy properties are correlated with the assembly times of their host halos.

Central galaxies of a given stellar mass with higher f_c

are found to be redder and more quenched in star formation while $f_c > 0.02$. This implies that star formation in centrals in this regime is dictated by their halo assembly history. A reversed albeit weak trend is seen for centrals with $f_c < 0.02$, which reflects the down-sizing effect that a more massive halo on average reaches the mass of most efficient *in situ* star formation, $\sim 10^{12} M_\odot$, earlier. Similar trends with f_c are found for the bulge to total ratio, B/T : central galaxies hosted by older halos tend to have higher B/T ratios. We suggest that this is because older halos are more compact and their formation is more dominated by major mergers. For a given stellar mass, the sizes of central galaxies are also correlated with f_c for both ellipticals (in terms of the half-light radius, R_{50}) and spirals (in terms of the disk scale-length, R_{disk}), with centrals hosted by older halos being smaller. This trend is again consistent with the fact that halos of a given mass are more compact at higher redshifts.

We have also analyzed how the intrinsic properties of satellite galaxies change with the value of f_c of their host halos. Here we found that, for a given stellar mass, satellites residing in older halos are redder and more quenched, and this trend is stronger for lower mass halos. Satellites also appear smaller than centrals of the same mass, and this is true for both ellipticals and spirals. These results can again be explained by the fact that halos that assembled earlier are more compact. As for centrals, a weak down-sizing effect in the quenching of star formation is also seen for satellites hosted by massive halos with $f_c < 0.02$. These results, together with those found for the centrals, demonstrate clearly that halo assembly plays an important role in determining the properties of galaxies the halos host.

We present our preliminary comparisons of our observational results with the predictions by the AAM model of [Hearin & Watson \(2013\)](#) and by the SAM of [Lu et al. \(2014a\)](#). The AAM model reproduces well the general trends in the observational data, while the SAM fails to do so. The SAM predicts too many quenched low-mass satellites and too small fraction of quenched high-mass galaxies. These imply that halo assembly history is another important factor in addition to halo mass that can affect star formation in galaxies, and such effects have yet to be properly modeled in the SAM. In this context, the observational results obtained here are expected to provide stringent constraints on theoretical models of galaxy formation and evolution. We will come back to detailed comparison between our observational results and model predictions in a forthcoming paper.

ACKNOWLEDGMENTS

We thank Andrew Hearin for help in using his mock catalog, Yu Lu for using his semi-analytical data, and Zhankui Lu for helpful discussion and the anonymous referee for helpful comments that greatly improved the presentation of this paper. HJM acknowledges the support from NSF AST-1109354. This work is also supported by the 973 Program (Nos. 2015CB857002, 2015CB857005).

REFERENCES

- Abazajian K. N. et al., 2009, *ApJS*, 182, 543
 Behroozi P. S., Conroy C., Wechsler R. H., 2010, *ApJ*, 717, 379
 Behroozi P. S. et al., 2013, *ApJ*, 763, 18
 Berlind A. A., Weinberg D. H., 2002, *ApJ*, 575, 587
 Blanton M. R. et al., 2005, *AJ*, 129, 2562
 Brinchmann J., Charlot S., White S. D. M., Tremonti C., Kauffmann G., Heckman T., Brinkmann J., 2004, *MNRAS*, 351, 1151
 Choi Y. Y., Han D. H., Kim S. S., 2010, *Journal of Korean Astronomical Society*, 43, 191
 Colless M. et al., 2001, *MNRAS*, 328, 1039
 Conroy C., Wechsler R. H., 2009, *ApJ*, 696, 620
 Dressler A., 1980, *ApJ*, 236, 351
 Gallazzi A., Charlot S., Brinchmann J., White S. D. M., Tremonti C., 2005, *MNRAS*, 362, 41
 Guo Q., White S. D. M., Li C., Boylan-Kolchin M., 2010, *MNRAS*, 404, 1111
 Hearin A. P., Watson D. F., 2013, *MNRAS*, 435, 1313
 Hearin A. P., Watson D. F., Becker M. R., Reyes R., Berlind A. A., Zentner A. R., 2014, *MNRAS*, 444, 729
 Jing Y. P., Mo H. J., Börner G., 1998, *ApJ*, 494, 1
 Kang X., Jing Y. P., Mo H. J., Börner G., 2005, *ApJ*, 631, 21
 Kauffmann G. et al., 2003, *MNRAS*, 341, 33
 Klypin A. A., Trujillo-Gomez S., Primack J., 2011, *ApJ*, 740, 102
 Kravtsov A. V., Berlind A. A., Wechsler R. H., Klypin A. A., Gottlöber S., Allgood B., Primack J. R., 2004, *ApJ*, 609, 35
 Kravtsov A. V., 2013, *ApJL*, 764, L31
 Leauthaud A. et al., 2012, *ApJ*, 744, 159
 Li Y., Mo H. J., van den Bosch F. C., Lin W. P., 2007, *MNRAS*, 379, 689
 Li Y., Mo H. J., Gao L., 2008, *MNRAS*, 389, 1419
 Lu Y., Mo H. J., Lu Z., Katz N., Weinberg M. D., 2014a, *MNRAS*, 443, 1252
 Lu Z., Mo H. J., Lu Y., Katz N., Weinberg M. D., van den Bosch F. C., Yang X., 2014b, *MNRAS*, 439, 1294
 Lu Z., Mo H. J., Lu Y., 2015, *MNRAS*, in press (arXiv:1408.2640)
 Mo H. J., Mao S., White S. D. M., 1999, *MNRAS*, 304, 175
 Mo H. J., van den Bosch F. C., White S. D. M., 2010, *Galaxy Formation and Evolution*. Cambridge University Press, New York, NY
 Moustakas J. et al., 2013, *ApJ*, 767, 50
 Neistein E., Weinmann S. M., Li C., Boylan-Kolchin M., 2010, *ArXiv:1011.2492*
 Peacock J. A., Smith R. E., 2000, *MNRAS*, 318, 1144
 Scoccimarro R., Sheth R. K., Hui L., Jain B., 2001, *ApJ*, 546, 20
 Seljak U., 2000, *MNRAS*, 318, 203
 Simard L., Mendel J. T., Patton D. R., Ellison S. L., McConnell A. W., 2011, *ApJS*, 196, 11
 Tinker J. L., Kravtsov A. V., Klypin A., Abazajian K., Warren M. S., Yepes G., Gottlöber S., Holz D. E., 2008, *ApJ*, 688, 709
 Tremonti C. et al., 2004, *ApJ*, 613, 898
 Vale A., Ostriker J. P., 2004, *MNRAS*, 353, 189
 Vale A., Ostriker J. P., 2006, *MNRAS*, 371, 1173

- van den Bosch F. C., Yang X., Mo H. J., 2003, MNRAS, 340, 771
- van den Bosch F. C., Yang X., Mo H. J., Weinmann S. M., Macciò A. V., More S., Cacciato M., Skibba R., Kang X., 2007, MNRAS, 376, 841
- Wang H., Mo H. J., Guo Y., van den Bosch F. C., Yang X., 2009, MNRAS, 394, 398
- Wang H., Mo H. J., Jing Y. P., Yang X., Wang Y., 2011, MNRAS, 413, 1973
- Wang H., Mo H. J., Yang X., van den Bosch F. C., 2012, MNRAS, 420, 1809
- Watson D. F., Berlind A. A., McBride C. K., Hogg D. W., Jiang T., 2012, ApJ, 749, 83
- Watson D. F., Hearin A. P., Berlind A. A., Becker M. R., Behroozi P. S., Skibba R. A., Reyes R., Zentner A. R., van den Bosch F. C., 2015, MNRAS, 446, 651
- Weinmann S. M., Kauffmann, G., van den Bosch F. C., Pasquali A., McIntosh D. H., Mo H. J., Yang X., Guo Y., 2009, MNRAS, 394, 1213
- Willett K. W. et al., 2013, MNRAS, 435, 2835
- Yang X., Mo H. J., van den Bosch F. C., 2003, MNRAS, 339, 1057
- Yang X., Mo H. J., Jing Y. P., van den Bosch F. C., Chu Y. Q., 2004, MNRAS, 350, 1153
- Yang X., Mo H. J., van den Bosch F. C., Jing Y. P., 2005, MNRAS, 356, 1293
- Yang X., Mo H. J., van den Bosch F. C., Pasquali A., Li C., Barden M., 2007, ApJ, 671, 153
- Yang X., Mo H. J., van den Bosch F. C., Zhang Y., Han J., 2012, ApJ, 752, 41
- Zhao D. H., Jing Y.P., Mo H.J., Börner G., 2009, ApJ, 707, 354
- Zheng Z., Coil A. L., Zehavi I., 2007, ApJ, 667, 760